International Journal of Electrical, Electronic and Communication Sciences
ISSN: 2517-9438
Vol:3, No:2, 2009

Bit-Error-Rate Performance Analysis of an Overlap-based CSS System

Taeung Yoon, Dahae Chong, Sangho Ahn, and Seokho Yoon

Abstract—In a chirp spread spectrum (CSS) system, the overlap technique is used for increasing bit rate. More overlaps can offer higher data throughput; however, they may cause more intersymbol interference (ISI) at the same time, resulting in serious bit error rate (BER) performance degradation. In this paper, we perform the BER analysis and derive a closed form BER expression for the overlap-based CSS system. The derived BER expression includes the number of overlaps as a parameter, and thus, would be very useful in determining the number of overlaps for a specified BER. The numerical results demonstrate that the BER derived in a closed form closely agrees with the simulated BER.

Keywords—CSS, DM, chirp, overlap.

I. Introduction

CHIRP spread spectrum (CSS) is a spread spectrum technique that uses chirp signals and the associated pulse compression method. Originally, CSS technology has been widely developed and deployed for military radar systems, and recently, due to its high processing gain, high time resolution, low power consumption, and anti-jamming and anti-multipath capabilities, there has been considerable interest in application of CSS to indoor wireless communication systems [1]: in March 2007, for example, the institute of electrical and electronics engineers (IEEE) has approved CSS physical layer (PHY) in its new wireless standard 802.15.4a, allowing CSS to be used in various applications such as real time location systems (RTLS), industrial control, sensor networking, and medical devices [2].

In CSS, a data signal is spread over a wider frequency band via chirp signals for transmission. CSS can be classified into two categories, depending on how to modulate chirp signals with data: one is binary orthogonal keying (BOK) and the other is direct modulation (DM). BOK uses chirp signals for representing data: for example, bits '1' and '0' can be represented by chirp signals with positive and negative instantaneous frequency change rates, respectively. On the other hand, DM uses a chirp signal just as a spreading code and performs data modulation and demodulation separately and independently from the chirp processing. Thus, DM can be incorporated with various modulation techniques [3]. In this paper, we consider the DM scheme.

Overlap is one of the techniques for increasing bit rate in CSS. More overlaps can offer higher data throughput; however, they may cause more intersymbol interference (ISI) at the same time, resulting in serious bit error rate (BER) performance degradation [1]. Thus, the number of overlaps should be set adequately according to the required BER performance, and in doing so, it would be very useful if there is a closed form BER expression that includes the number of overlaps as a parameter. In [3], it was mentioned that the BER performance of overlap-based CSS systems changes according to the number of overlaps; however, no mathematical analysis or no closed form associated with BER is presented.

T. Yoon, D. Chong, S. Ahn, and S. Yoon are with the School of Information and Communication Engineering, Sungkyunkwan University, Suwon, 440-746, Korea (e-mail: syoon@skku.edu)

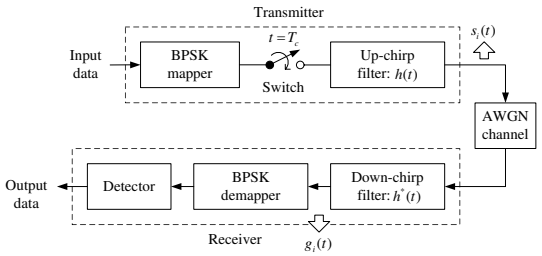

Fig. 1. Block diagram of the DM-BPSK system.

In this paper, thus, we are to derive a closed form expression for BER of the overlap-based CSS systems, exploiting the approximated Gaussian Q function [4]. The remainder of this paper is organized as follows. In Section II, the overlap-based CSS system model is described. Section III derives a closed form BER expression of the overlap-based CSS system, and investigates parameter values to improve the accuracy of the approximated Gaussian Q function (and consequently, to enhance that of the derived analytical BER). In Section IV, the analytic results are verified by BER performance simulation and finally Section V concludes this paper.

II. System Model

The complex baseband equivalent $c(t)$ of a typical linear chirp waveform is expressed as

$$c(t) = \sqrt{\frac{1}{T_c}} \exp(j\pi\mu t^2), \quad |t| < \frac{T_c}{2}, \tag{1}$$

where T_c and μ $(\neq 0)$ denote chirp duration and chirp rate, respectively. The chirp rate is defined as the change rate of an instantaneous frequency. A chirp signal is called the up-chirp (down-chirp) signal when μ is positive (negative), where instantaneous frequency increases (decreases). We consider a DM binary phase shift keying (BPSK) system with the up-chirp as shown in Fig. 1. In the Fig. 1, input binary data stream is first mapped according to the BPSK mapping rule. Next, mapper output signal is modulated into a short intermediate frequency (IF) pulse every T_c seconds. The phase

modulated IF pulse passes through an up-chirp filter with impulse response $h(t) = \sqrt{\frac{1}{T_c}}\exp(j\pi\mu t^2)$, where $\mu > 0$ and $|t| < \frac{T_c}{2}$, then we can obtain the i-th transmitted DM-BPSK chirp symbol $s_i(t)$ expressed as

$$s_i(t) = b_i\sqrt{E_b}c(t), \quad i = \cdots, -2, -1, 0, 1, 2, \cdots \tag{2}$$

where E_b and $b_i \in \{\pm 1\}$ denote the transmitted signal energy per data bit and the i-th transmitted data bit, respectively. In the receiver, the disturbed signal by additive white Gaussian noise (AWGN) is first led to a down-chirp filter whose impulse response is $h^*(t) = \sqrt{\frac{1}{T_c}}\exp(j\pi\mu' t^2)$, where $\mu' = -\mu$ and $|t| < \frac{T_c}{2}$. The i-th down-chirp filter output $g_i(t)$, which is compressed sinc-like pulse-shaped signal with much narrower main lobe width, is given by [5]

$$\begin{aligned} g_i(t) = s_i(t) \otimes h^*(t) &= b_i(\sqrt{E_b})\frac{\sin\left\{\pi Bt\left(1 - \frac{|t|}{T_c}\right)\right\}}{\pi Bt} \\ &= b_i(\sqrt{E_b})p(t), \quad |t| < T_c, \end{aligned} \tag{3}$$

where B ($\triangleq |\mu|T_c$) is the chirp bandwidth defined as the range of the instantaneous frequency, '$\otimes$' denotes the convolution operation, and $p(t) = \sin\{\pi Bt(1 - |t|/T_c)\}/\pi Bt$. The envelope of $g_i(t)$ in (3) passes through the first zero points at $t \approx \pm\frac{1}{B}$. Therefore, the compression ratio or processing gain (defined as the ratio of chirp duration to the pulse width of $g_i(t)$) is given by BT_c [5]. After the down-chirp filtering, the compressed signal is sampled at $t = 0$, where $g_i(t)$ is maximized, and demapped. Finally, the output data is determined either '0' or '1' according to the demapping result.

If we transmit the overlapped chirp signal, the received signal is also overlapped. Thus, we can express the overlapped version $s_i^{overlap}(t)$ of $s_i(t)$ and the corresponding received signal $r(t)$ as

$$s_i^{overlap}(t) = \sum_{k=-(O_f-1)}^{O_f-1} s_{i+k}(t + k\tau) \tag{4}$$

and

$$r(t) = s_i^{overlap}(t) + w(t), \tag{5}$$

respectively, where O_f, τ ($= T_c/O_f$), and $w(t)$ denote the number of overlaps, overlap interval between chirp symbols, and a Gaussian distributed noise with mean zero and two-sided power spectral density $N_0/2$, respectively. The i-th down-chirp filter output $g_i^{overlap}(t)$ of the overlapped received signal sampled at $t = 0$ can be expressed as

$$\begin{aligned} g_i^{overlap}(t)|_{t=0} &= r(t) \otimes h^*(t)|_{t=0} \\ &= \sum_{k=-(O_f-1)}^{O_f-1} g_{i+k}(k\tau) + n \\ &= (\sqrt{E_b}) \sum_{k=-(O_f-1)}^{(O_f-1)} b_{i+k}p(k\tau) + n, \end{aligned} \tag{6}$$

where n ($= w(t) \otimes h^*(t)|_{t=0}$) denotes a filtered noise component with mean zero and variance $N_0/2$.

III. BER Analysis and Closed Form BER Expression

Since b_i takes on +1 or -1 with equal probability and Gaussian probability density function (pdf) is symmetric about zero, we can express the bit error probability P_B as

$$\begin{aligned} P_B &= \frac{1}{2}\{Pr(g_i^{overlap}(0) < 0 | b_i = 1) \\ &\quad + Pr(g_i^{overlap}(0) > 0 | b_i = -1)\} \\ &= Pr(g_i^{overlap}(0) > 0 | b_i = -1). \end{aligned} \tag{7}$$

Let us denote the normalized ISI z_i in $g_i^{overlap}(t)$ by

$$z_i = \sum_{\substack{k=-(O_f-1) \\ k\neq 0}}^{(O_f-1)} z_k, \tag{8}$$

where z_k ($= b_{i+k}p(k\tau)$) represents the ISI component due to $s_{ith}(t)$. Using (6), (7), and (8), we can express the bit error probability $P_B|_{z_i}$ conditioned on z_i as follows:

$$\begin{aligned} P_B|_{z_i} &= Pr\{n > (\sqrt{E_b} - \sqrt{E_b}z_i)\} \\ &= \frac{1}{\sigma\sqrt{2\pi}} \int_{(\sqrt{E_b})(1-z_i)}^{\infty} \exp\left(-\frac{t^2}{2\sigma^2}\right) dt \\ &= Q\left(\sqrt{\frac{2E_b}{N_0}}(1 - z_i)\right), \end{aligned} \tag{9}$$

where $Q(x)$ ($= \frac{1}{\sqrt{2\pi}}\int_x^\infty e^{-t^2/2}dt$) and σ are the Gaussian Q function and the standard deviation of noise component n, respectively. Thus, the unconditional bit error probability P_B can be obtained as

$$P_B = \mathbf{E}_{z_i}\left\{Q\left(\sqrt{\frac{2E_b}{N_0}}(1 - z_i)\right)\right\}, \tag{10}$$

where $\mathbf{E}_{z_i}\{\cdot\}$ denotes the expectation over z_i. As shown in (10), to derive a closed form expression for P_B, we need to average Q function over the pdf of z_i, however, which should be highly complicated, if not possible. Thus, we employ the following approximation (denoted by $\hat{Q}$) for the Gaussian Q function, which can be obtained based on series of exponentially decreasing cosine (EDC) [4]:

$$\begin{aligned} \hat{Q}(x) &= \sum_{m=0}^{N_T-1} c_m e^{\lambda_m x}\cos(\omega_m x) \\ &= \mathbf{Re}\left[\sum_{m=0}^{N_T-1} c_m e^{(\lambda_m + j\omega_m)x}\right], \end{aligned} \tag{11}$$

where N_T is a given length of series, $\mathbf{Re}\{\cdot\}$ is the real operator, and c_m, λ_m, and ω_m are real-valued parameters subject to the constraint that the following symmetric squared relative error (SSRE) ϵ between $Q(x)$ and $\hat{Q}(x)$ is minimized [6]:

$$\begin{aligned} \epsilon &= \int_\chi \left[1 - \frac{\hat{Q}(x)}{Q(x)}\right]^2 + \left[1 - \frac{Q(x)}{\hat{Q}(x)}\right]^2 dx \\ &\simeq \frac{1}{N_s}\sum_{i=1}^{N_s}\left[1 - \frac{\hat{Q}(x_i)}{Q(x_i)}\right]^2 + \left[1 - \frac{Q(x_i)}{\hat{Q}(x_i)}\right]^2, \end{aligned} \tag{12}$$

where the formula in the second row of (12) is the discrete expression of the integral form in the first row and χ and N_s represent the range of the argument x over which we wish to minimize ϵ and the total number of samples over χ, respectively. Substituting (8) and (11) into (10), we can rewrite P_B as follows:

$$\begin{aligned} P_B &\simeq \mathbf{E}_{z_i}\left\{\hat{Q}\left(\sqrt{\frac{2E_b}{N_0}}(1-z_i)\right)\right\} \\ &= \mathbf{Re}\Bigg[\sum_{m=0}^{N_T-1} c_m e^{(\lambda_m+j\omega_m)\sqrt{\frac{2E_b}{N_0}}} \\ &\quad \times \mathbf{E}_{z_i}\left\{e^{-(\lambda_m+j\omega_m)\sqrt{\frac{2E_b}{N_0}}z_i}\right\}\Bigg] \\ &= \mathbf{Re}\Bigg[\sum_{m=0}^{N_T-1} c_m e^{(\lambda_m+j\omega_m)\sqrt{\frac{2E_b}{N_0}}} \\ &\quad \times \prod_{\substack{k=-(O_f-1)\\ k\neq 0}}^{(O_f-1)} M_{z_k}\left(-(\lambda_m+j\omega_m)\sqrt{\frac{2E_b}{N_0}}\right)\Bigg], \end{aligned} \tag{13}$$

where $M_{z_k}(t)$ ($\triangleq \mathbf{E}_{z_k}\{e^{tz_k}\}$) is the moment generating function (MGF) of z_k. Since $z_k = \{\pm p(kT_c/O_f)\}$, $M_{z_k}(t)$ can be represented as

$$\begin{aligned} M_{z_k}(t) &= \frac{1}{2}\left\{e^{tp(kT_c/O_f)} + e^{-tp(kT_c/O_f)}\right\} \\ &= \cosh\left\{p\left(k\frac{T_c}{O_f}\right)t\right\}. \end{aligned} \tag{14}$$

After the substitution of (14) into (13), finally, we get a closed form BER expression for the DM-BPSK system:

$$\begin{aligned} P_B \simeq \mathbf{Re}\Bigg[\sum_{m=0}^{N_T-1} c_m e^{(\lambda_m+j\omega_m)\sqrt{\frac{2E_b}{N_0}}} \prod_{\substack{k=-(O_f-1)\\ k\neq 0}}^{(O_f-1)} \\ \cosh\left\{p\left(k\frac{T_c}{O_f}\right)(\lambda_m+j\omega_m)\sqrt{\frac{2E_b}{N_0}}\right\}\Bigg]. \end{aligned} \tag{15}$$

Meanwhile, due to the non-linear characteristic and fast decay rate of the Gaussian Q function, the wider range of $Q(x)$ dealt with is, the larger N_T (and thus, more parameters) is required in order to guarantee the specified accuracy of the $\hat{Q}(x)$ over the whole range of interest, which makes the use of $\hat{Q}(x)$ impractical. To solve this problem, we first divide the whole BER range of interest (which is set from 0.5 to 10^{-10}, in this paper) into two segments, one is set from 0.5 to 10^{-3} and the other is set from 10^{-3} to 10^{-10} (the segment range might be set differently from that in this paper, which was found to have little effect on the result). Then, length (N_T) and parameters (c_m, λ_m, and ω_m) of $\hat{Q}(x)$ that satisfy the target SSRE (which is set to 0.01 in this paper) are obtained numerically over χ corresponding to each segment, where 1000 samples (i.e., N_s=1000) obtained uniformly over χ were used. The obtained results are shown in Tables I and II. From the tables, we can see that 30 parameters are required to achieve the target SSRE. On the other hand, the target SSRE was not able to be satisfied even with 33 parameters (i.e., N_T=11) when one single series is used. Thus two shorter EDC series are used for the computation $\hat{Q}(x)$, instead of a longer EDC series.

TABLE I
PARAMETERS FOR $\hat{Q}(x)$ OVER THE BER RANGE FROM 0.5 TO 10^{-3} WHEN THE TARGET SSRE IS 0.01 ($N_T = 3$).

m	c_m	λ_m	ω_m
0	-5.498493	-2.394775	1.155583×10^{-1}
1	4.165956	-2.132909	3.038220×10^{-1}
2	1.483053	-1.957114	-4.425860×10^{-1}

TABLE II
PARAMETERS FOR $\hat{Q}(x)$ OVER THE BER RANGE FROM 10^{-3} TO 10^{-10} WHEN THE TARGET SSRE IS 0.01 ($N_T = 7$).

m	c_m	λ_m	ω_m
0	-6.800443×10^{-1}	-2.639689	1.020882
1	-3.237126×10^{-1}	-2.696018	2.670366×10^{-2}
2	-1.595907×10^{-2}	-2.110599	-1.528960×10^{-1}
3	-7.330517	-3.314070	-1.167062
4	1.984192	-2.960136	1.449151×10^{-1}
5	2.390374	-2.818848	7.848084×10^{-3}
6	-1.639812	-2.919649	1.453802

IV. NUMERICAL RESULTS

In this section, we compare the *theoretical* BER of the overlap-based CSS systems derived in a closed form in this paper with the *empirical* BER. We assume that the sampling time synchronization is perfect. The chirp duration (T_c), rate (μ), and bandwidth (B) are set to 0.5 μs, 400 MHz/μs, and 200 MHz, respectively. For the computation of $\hat{Q}(x)$, the parameter values represented in Tables I and II are used.

Fig. 2 shows the theoretical BER performance comparison between BPSK and DM-BPSK when there is no overlap ($O_f = 1$), where BPSK and DM-BPSK BER curves were plotted using (9) and (15). As shown in the figure, the two BERs are almost same, which stems from the fact that data

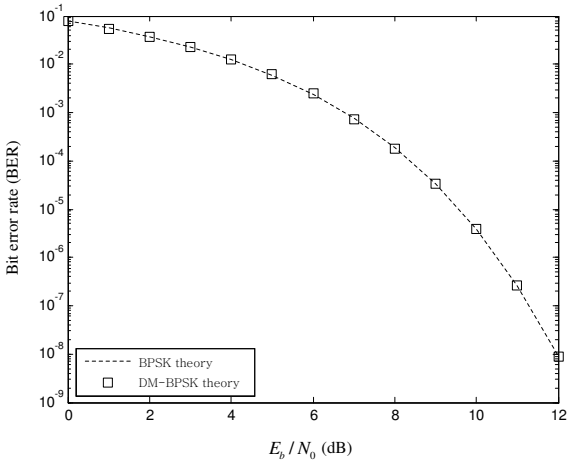

Fig. 2. Theoretical BER performance comparison between BPSK and DM-BPSK when there is no overlap ($O_f = 1$).

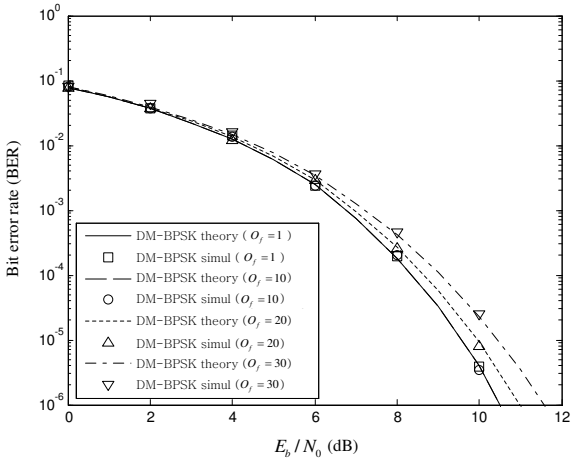

Fig. 3. Theoretical and simulated BER curves of the overlap-based DM-BPSK for various values of O_f.

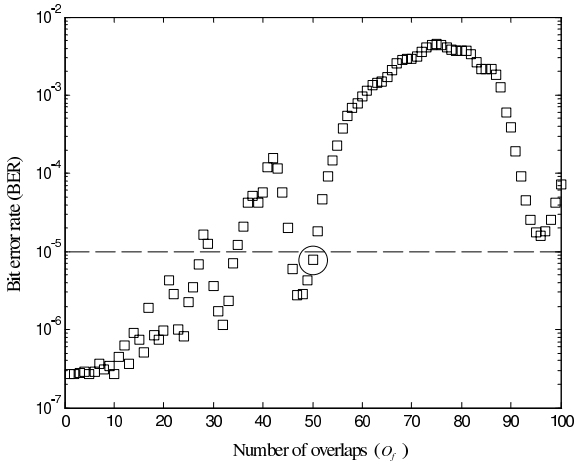

Fig. 4. BER performance for the DM-BPSK system as a function of the number of overlaps when $E_b/N_0 = 11$dB.

modulation and demodulation are performed separately and independently from the chirp processing in DM, and implies the approximation $\hat{Q}(x)$ for Q function is reliable.

Fig. 3 shows the theoretical and simulated BER curves of the overlap-based DM-BPSK for various values of O_f. In the figure, we can clearly see a close agreement between the theoretical BER based on $\hat{Q}(x)$ and simulated BER based on Monte Carlo runs. Another important observation is that there is little BER performance difference between two cases that $O_f = 1$ and $O_f = 10$. This is because the down-chirp filter output in (3) has a very narrow mainlobe width. Even if several down-chirp filter outputs are overlapped, there will be little ISI in the down-chirp filter output of interest when the overlap interval $\tau\ (= T_c/O_f)$ is much wider than the mainlobe width of the down-chirp filter output. When $O_f = 10$, the overlap interval between chirp symbols is $50\ ns$ (=0.5 $\mu s/10$), which is about 5 times wider than the mainlobe width of the down-chirp filter output of $10\ ns$ (=$2/B$). Therefore, BER performance degradation due to ISI is not significant when $O_f = 10$; however, it becomes pronounced as O_f increases as shown in the figure.

Fig. 4 shows how the BER performance changes according to the number of overlaps, which was plotted using the derived BER expression (15). This figure can help us determine the number of overlaps satisfying a required system BER performance. For example, let us assume that the required BER limit for a reliable transmission is set to 10^{-5} (dotted line). In the figure, we can find that the maximum allowable number of overlaps among these overlaps is 50 (circled line). Thus, if we use this number of overlaps, we can increase data rate as much as possible with satisfying the given BER constraint. From this figure, we can also observe that more overlaps do not always cause more performance degradation. This is because that the down-chirp filter output is a sinc-like function with multiple zero-crossing points. Although several down-chirp filter outputs are overlapped, there will be no ISI in the down-chirp filter output of interest when the sampling time for the down-chirp filter output of interest coincides with zero-crossing points of other down-chirp filter outputs. On the other hand, though, the down-chirp filter output of interest can be strongly influenced by ISI caused by other down-chirp filter outputs when its sampling time does not correspond to zero-crossing points of other down-chirp filter outputs. Therefore, we can deduce that the degree of BER performance degradation due to ISI is not linearly proportional to the number of overlaps.

V. Conclusion

In this paper, a closed form BER expression has been obtained based on the approximated Gaussian Q function for the overlap-based CSS systems. For the computation of the approximated Gaussian Q function, instead of a longer EDC series, two shorter EDC series and the associated parameters are presented, which make the derived closed form BER expression more feasible. The numerical results have shown that the BER derived in a closed form closely agrees with the simulated BER. The closed form BER expression derived in this paper should be very useful in determining the number of overlaps according to a required system performance in the overlap-based CSS systems.

Acknowledgment

This work is the outcome of a Manpower Development Program for Energy & Resources supported by the Ministry of Knowledge and Economy (MKE).

References

[1] P. Zhang and H. Liu, "An ultra-wide band system with chirp spread spectrum transmission technique," in *Proc. Int. Conf. Intelligent Tutoring Systems (ITS)*, pp. 294-297, Jhongli, Taiwan, June 2006.
[2] IEEE Std. 802.15.4a-2007, *Wireless MAC and PHY Specifications for Low-Rate Wireless Personal Area Networks (WPANs)*, IEEE, 2007.
[3] J. Pinkney, *Low Complexity Indoor Wireless Data Links Using Chirp Spread Spectrum*, Ph. D. Dissertation, Dept. Elect. Comput. Engineer., University of Calgary, Calgary, Canada, 2003.
[4] O. Fonseca and I. N. Psaromiligkos, "BER performance of BPSK transmissions over multipath channels," *Electron. Lett.*, vol. 42, no. 20, pp. 1164-1165, Sep. 2006.

[5] A. Springer, W. Gugler, M. Huemer, R. Koller, and R. Weigel, "A wireless spread-spectrum communication system using SAW chirped delay lines," *IEEE Trans. Microwave Theory Tech.*, vol. 49, no. 4, pp. 754-760, Apr. 2001.
[6] O. Fonseca and I. N. Psaromiligkos, "Approximation of the bit-error-rate of BPSK transmissions over frequency selective channels," in *Proc. IEEE Int. Conf. Wireless and Mobile Computing, Networking and Commun. (WiMob)*, pp. 217-222, Montreal, QB, Canada, Aug. 2005.

Taeung Yoon received the B.S.E. degree in the School of Information and Communication Engineering from Sungkyunkwan University, South Korea, in 2008. He is currently working towards his M.S.E. degree in the Digital Communications laboratory under Prof. Seokho Yoon. His current research interests are single carrier frequency division multiple access (SC-FDMA), multiple-input multiple-output (MIMO) systems, and cooperative wireless communications. Mr. Yoon was the recipient of the Grand paper award at IEEE Seoul section student paper contest 2008.

Dahae Chong received the B.S.E. and M.S.E. degrees in electronic and electrical engineering from Sungkyunkwan University, South Korea, in 2006 and 2008, respectively. He is currently working towards the Ph. D. degree in the Department of Mobile Systems Engineering at Sungkyunkwan University. He has been a teaching and research assistant at the school of information and communication engineering, Sungkyunkwan University, since March 2006. His research interests include ultra-wideband (UWB) communications, cognitive radio, and cooperative communications.

Sangho Ahn received the B.S.E. degree in electrical engineering from Sungkyunkwan University, Suwon, Korea, in 2007. He received the best paper award from the School of Information and Communication Engineering in Sungkyunkwan University, 2007. Currently, he is working toward the M.S.E. degree in electrical engineering at Sungkyunkwan University. His current research interests include orthogonal frequency division multiplexing (OFDM), and cooperative communication.

Seokho Yoon received the B.S.E. (*summa cum laude*), M.S.E., and Ph.D. degrees in electrical engineering from Korea Advanced Institute of Science and Technology, Daejeon, Korea, in 1997, 1999, and 2002, respectively. From April 2002 to June 2002, he was with the Department of Electrical Engineering and Computer Science, Massachusetts Institute of Technology, Cambridge. From July 2002 to February 2003, he was with the Department of Electrical Engineering, Harvard University, Cambridge, as a Postdoctoral Research Fellow. In March 2003, he joined the School of Information and Communication Engineering, Sungkyunkwan University, Suwon, Korea, where he is currently an Assistant Professor. His research interests include spreadspectrum systems, mobile communications, detection and estimation theory, and statistical signal processing. Dr. Yoon is a member of the Institute of Electronics Engineers of Korea and the Korean Institute of Communication Sciences. He received the Bronze Prize at the Samsung Humantech Paper Contest in 2000.